

An analysis of micro- and macro-vasculature blood flow characteristics during graded stimulation

Y-C. L. Ho^{1,2}, E. T. Petersen^{1,2}, X. Golay^{1,3}

¹Neuroradiology, National Neuroscience Institute, Singapore, Singapore, ²BioEngineering, Nanyang Technological University, Singapore, Singapore, Singapore, ³Singapore Bioimaging Consortium, A*STAR, Singapore, Singapore, Singapore

Introduction:

Arterial spin labeling has been used in a number of studies to directly measure the perfusion changes upon stimulation [1]. A major difference among all these studies, especially those using pulsed ASL sequences, comes from their use – or not – of crusher gradients to avoid vascular effects [2-4]. Recently, a method for obtaining information on both macro- and microvascular blood flow has been introduced, using arterial spin labeling with and without crusher gradients [5]. This method shows the advantage of detecting information on both arrival times for the arterial system (τ_a) and microvasculature (τ_m) independently. This is important, because traditional CBF estimation relying on single-compartment kinetics and single time-point acquisition needs to assume unchanging arrival times, while it is probable that at least the transit time to the microvasculature will be changed under activation [3]. In this study, we used the recently developed QUASAR sequence [5] to derive a model-free estimation of CBF and arterial blood volume (aBV), and to detect changes in arterial and microvasculature arrival times upon visual stimulation.

METHODS: Experiments: Studies were performed on a clinical 3.0T imager (Philips Medical Systems). Six healthy subjects (5 males, 1 female; mean age 29.7±1.6) were presented with graded visual stimuli and scanned using the QUASAR sequence [5]. Informed consent was obtained. **MR parameters:** ASL sequence parameters: slices=1, thickness=5 mm, gap=1 mm, $\alpha=27^\circ$, TR/TE₁=3000/23 ms, $\Delta TI=100$ ms, time points=26, SENSE factor=3, labeling slab=150 mm, inversion gap=30 mm, crusher encoding velocity $V_{enc}=[\infty, 3$ cm/s]. A single slice was acquired along the calcarine sulcus to image the primary visual area. The functional paradigm was a gray-white, 8Hz visual checkerboard pattern (3 levels of contrast – 25%, 50%, 100%) that alternated with a baseline condition (iso-luminance gray (50%) background). Two types of runs were acquired: with crusher gradients and 10 baseline blocks (15 volumes each) alternating with 9 visual blocks (10 volumes each); and without and 4 baseline blocks alternating with 3 visual blocks. **Data Analysis:** The functional images were realigned if necessary. Linear interpolation of the control and labelled data was done separately before pair-wise subtraction to avoid BOLD effects [6]. Tissue curves, $\Delta M(t)$ for visual contrasts and baseline conditions were then derived from the crushed and non-crushed data on a voxel-by-voxel basis for each volume. RS-tests ($p<0.001$, uncorrected) were performed on a voxel-by-voxel basis to determine the regions of interest (ROIs). Within each subject, only the commonly activated voxels were selected for further analysis. To quantify CBF changes during activation and to derive the various arrival times, we used [7]:

$$\Delta M = 2 \cdot M_{a,0} \cdot f \cdot \int_0^t c(\tau) \cdot r(t-\tau) \cdot m(t-\tau) d\tau$$

is the flow, $c(t)$ is the AIF, $r(t-\tau)$ is the residue function describing the clearance of spin from the tissue and $m(t-\tau)$ describes the longitudinal magnetization relaxation. The first 3 volumes of each visual block and the first 5 volumes of each baseline block were excluded from the analyses to ensure steady-state measurements. The tissue curves were then averaged across volumes in identical conditions to increase SNR. Arterial Input Functions [AIF(t) = $2 \cdot M_{a,0} \cdot c(t)$] specific to each condition were estimated by subtraction of crushed from non-crushed tissue curves. τ_a and τ_m were estimated by detecting rising edges on AIFs and crushed tissue curves respectively. The AIFs were then scaled using M_0 (from sagittal sinus), inversion efficiency $\alpha=1.0$, and the correction factor of $n=(\tau_m \cdot \tau_a) / \Delta TI$ (due to multiple saturation phases experienced by the labeled blood). Circular singular value decomposition (C-SVD) was performed for the deconvolution of the crushed tissue curve by the AIF in order to calculate CBF. aBV was derived by estimating the area under the AIF curve.

RESULTS & DISCUSSION: All ROIs showed increases of CBF (mean 10.7 to 30.3%) and aBV (mean 11.4 to 29.1%) from baseline with rising stimulation, while τ_a , τ_m and τ_{m-a} decreased with increasing stimulation (see Table 1). These results confirm in part what other studies [2,3] have observed, while providing a broader range of information. In particular, the direct comparison between arterial and microvascular arrival times shows that, while τ_a decreases during stimulation, it is not as marked as that of τ_m (reflected in τ_{m-a}). Results are plotted in Figures 2 & 3. This fact possibly reflects the importance of the microvasculature in influencing delivery of oxygenated blood to the parenchyma during activity. During activation, flow velocity may increase in both large and small vasculature, as observed in transcranial Doppler studies [8] and studies on T1-dependent effects in BOLD-fMRI [9]. Hence, it is important to consider these dynamic parameters when modeling CBF, to avoid larger errors in CBF estimation. Given the consistency within subjects of the decrease in arrival times during stimulation, it could also be possible to use that as a parameter in the detection of activation. Considering the significantly changing arrival times, the CBF % changes of up to 30% are relatively muted. One possibility is that water is not exchanging fast enough in the capillaries and is simply being washed out of the microvasculature. Few studies have looked at aBV during activation. Here, we observe a consistent increase in aBV with respect to baseline, especially with increasing visual contrast (paired-t=2.68, df=5, $p<0.05$ at highest contrast condition). This is of interest, as it is thought that the larger vessels (>200 μ m) are not involved in regulating local haemodynamics during neuronal activity [10]. Our aBV estimations should reflect the volume of delivered blood only via the arteries and arterioles in the relevant voxels, although it is difficult to determine if there was absolutely no microvascular contribution. Overall, we have seen graded increases of CBF and aBV and graded decreases in τ_a and especially for τ_m , which have significant implications for CBF quantification. Of potential interest is also the idea of a washout effect in the capillaries, which could explain the intriguing relationship observed here of increased blood velocities (from shorter transit times) and relatively muted CBF changes.

REFERENCES: [1] Golay X. et al (2004) *TMRI* 15:255-265. [2] Gonzalez-At J.B. et al (2000) *MRM* 46:974-984. [3] Yang Y. et al (2000) *MRM* 44:680-685. [4] Hendrikse J. et al (2003) *MRM* 50:429-433. [5] Petersen E.T et al (2005) *MRM* (in press). [6] Lu H. et al (2005) *ISMRM* 35. [7] Buxton R.B. et al (1998) *MRM* 40:383-396. [8] Panczel G. et al (1999) *Stroke* 30:619-623. [9] Gao J.H. et al (1996) *MRM* 36:314-319. [10] Kruschinski W. (1996) *Regulation of CBF*: 245-262.

	CBF (ml/100g/min)	aBV (%)	τ_a (msec)	τ_m (msec)	τ_{m-a} (msec)
Baseline	94 ± 11	1.03 ± 0.1	367 ± 41	883 ± 90	517 ± 63
25% VC	104 ± 22	1.15 ± 0.2	328 ± 40	706 ± 74	378 ± 48
50% VC	109 ± 19	1.33 ± 0.2	294 ± 44	650 ± 58	356 ± 28
100% VC	122 ± 18	1.33 ± 0.2	311 ± 39	617 ± 69	306 ± 44

Table 1: CBF, aBV, τ_a , τ_m and τ_{m-a} values for each of the conditions (means and standard errors across subjects). Note that CBF standard errors here are relatively large since absolute values vary across subjects.

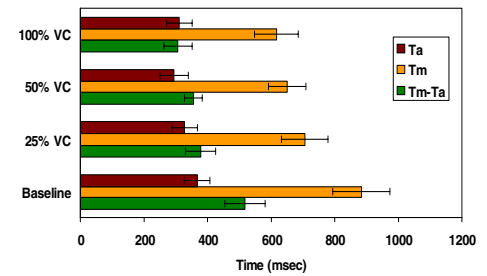


Figure 2: Mean τ_a , τ_m and τ_{m-a} for each of the visual contrast and baseline conditions.

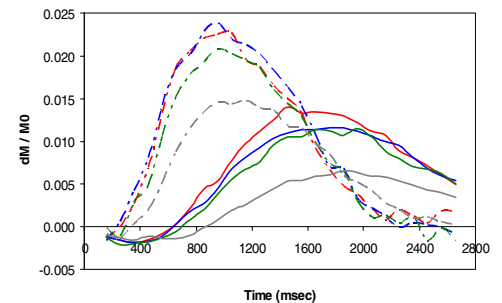


Figure 3: Tissue curves (solid lines) and fractional AIFs (broken lines) for each of the visual contrast and baseline conditions. Red lines – 100% visual contrast (VC) condition; blue – 50% VC; green – 25% VC; grey – baseline.